

## **(n, $\alpha$ ) reactions cross section research at IPPE.**

Khryachkov V.A.<sup>1,a</sup>, Bondarenko I.P.<sup>1</sup>, Kuzminov B.D.<sup>1</sup>, Semenova N.N.<sup>1</sup>, Sergachev A.I.<sup>1</sup>,  
Ivanova T.A.<sup>1,2</sup>, Giorginis G.<sup>3</sup>

<sup>1</sup>IPPE, Institute of Nuclear Physics Problems in Nuclear Engineering, 249033 Obninsk, Russia

<sup>2</sup>National Research Nuclear University MEPhI, Obninsk Institute for Nuclear Power Engineering of NRNU MEPhI, Obninsk, Russia.

<sup>3</sup>EU JRC – Institute for Reference Material and Measurements, Geel, Belgium.

**Abstract.** An experimental set-up based on an ionization chamber with a Frisch grid and wave form digitizer was used for (n, $\alpha$ ) cross section measurements. Use of digital signal processing allowed us to select a gaseous cell inside the sensitive area of the ionization chamber and determine the target atoms in it with high accuracy. This kind of approach provided us with a powerful method to suppress background arising from the detector structure and parasitic reactions on the working gas components. This method is especially interesting to study neutron reactions with elements for which solid target preparation is difficult (noble gases for example). In the present experiments we used a set of working gases which contained admixtures of nitrogen, oxygen, neon, argon and boron. Fission of <sup>238</sup>U was used as neutron flux monitor. The cross section of the (n, $\alpha$ ) reaction for <sup>16</sup>O, <sup>14</sup>N, <sup>20</sup>Ne, <sup>36</sup>Ar, <sup>40</sup>Ar and the yield ratio  $\alpha_0/\alpha_1$  of <sup>10</sup>B(n, $\alpha_0$ ) to <sup>10</sup>B(n, $\alpha_1$ ) reactions was measured for neutron energies between 1.5 and 7 MeV. Additionally a measurement of the <sup>50</sup>Cr(n, $\alpha$ ) cross section using a solid chromium target is also reported.

### **1 Experimental set up for gaseous targets**

A new spectrometer based on an ionization chamber with a Frisch grid and digital signal processing together with fast neutron beam profiling techniques were developed in collaboration between IRMM and IPPE. This spectrometer allows to measure (n, $\alpha$ ) reaction cross sections on working gas components with high precision [1]. The same type of setup was built at IPPE and in comparison with the IRMM one a set of improvements was achieved. Specifically the new setup allows to: 1) reliably suppress recoil proton background produced in hydrogenous working gases; 2) determine the directionality of  $\alpha$  particle emission; 3) work with electronegative working gases; 4) determine the pulse height defect for a set of light detector gases and compensate for it using a new method; 5) develop a novel technique for the measurement of the angular distribution of the reaction products.

---

<sup>a</sup> e-mail : [hva@ippe.ru](mailto:hva@ippe.ru)

All these improvements allowed us to extend the list of working gases and the number of elements which can be investigated.

The block diagram of the setup is shown in figure 1. The detector consists of two ionization chambers. The main ionization chamber with a Frisch grid (GIC) was used as spectrometer for  $(n,\alpha)$  reaction products. An additional parallel plate chamber which contains a thin solid  $^{238}\text{U}$  layer was used as neutron flux monitor. The uranium target was installed in a back-to-back geometry to the main chamber (main and monitor chambers have a common cathode). This allowed an accurate determination of the neutron flux at the target sample. The additional advantage of the common cathode is that the dead time for the main and monitor chambers is identical because the signal which triggers the registration of events is the same for both chambers.

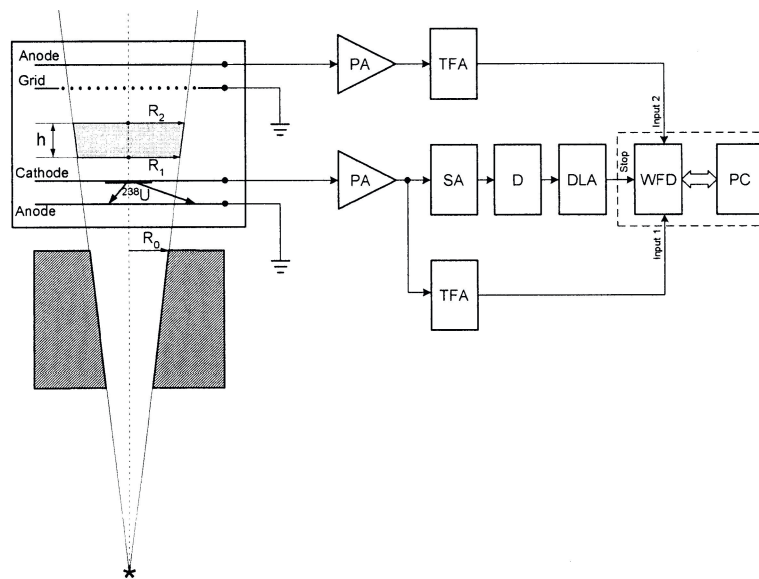


**Fig 1.** Block diagram of the experimental setup. PA – preamplifier, TFA – Timing filter amplifier, D – discriminator, SA – spectroscopy amplifier, DLA – Delay line amplifier, WFD – Waveform digitizer, PC – Personal computer.

The diameter of the electrodes was 12 cm, the distances cathode-to-grid and grid-to-anode were 40 and 3 mm, respectively. The axis of the neutron beam coincided with the symmetry axis of the GIC. Different isotopes existing in the working gas of the ionization chamber can contribute to the anode and cathode signals. The anode signal of the GIC and the common cathode signal at the exit of the corresponding charge sensitive preamplifiers were linearly amplified (without shaping) and fed to the inputs of a two channel waveform digitizer (WFD, LeCroy 2262, 10 bit). The digitization rate was 80 MHz or equivalently a signal sample was taken every 12.5 ns. The required trigger for the WFD operation was obtained by splitting the cathode signal after the preamplifier. The WFD was operated in the so called pre-trigger mode. Digitization was started by the DAQ (data acquisition programme) and the WFD memory was continuously filled till a trigger occurred. At this moment the memory contents were frozen and sent for storage to the PC hard disk. Typical digitised signals of an  $\alpha$  particle and a fission fragment can be seen in figure 2. They contain all needed information for the production of clean signatures of  $(n,\alpha)$  reactions on the working gas components and  $^{238}\text{U}$  fission, which are conditions for accurate cross section measurements.

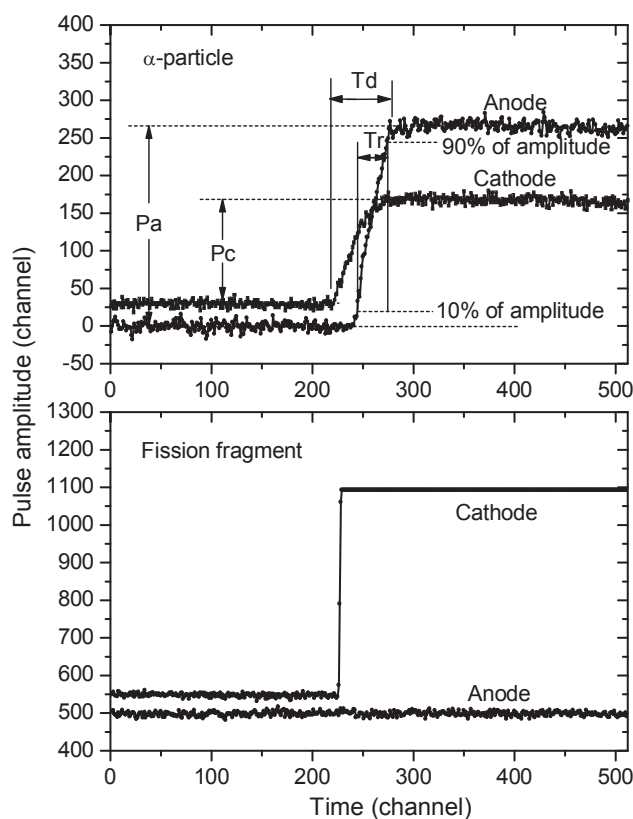


**Fig 2.** Examples of signals of the main (top) and monitor (bottom) chambers

Digital processing of the anode and cathode signals for each event provides information about the: 1) signal amplitude; 2) signal start time; 3) signal end time. Joint analysis of these parameters for each event allows to determine the: 1) total kinetic energy of the reaction products; 2) full electron drift time ( $T_d$ ) which can be transformed to a spatial (position) coordinate in the interelectrode space where the reaction took place; 3) anode signal rise time ( $T_r$ ) which can be used to obtain the emission angle of the light particle in the laboratory coordinate system; 4) shape of anode signal containing information about the particle type and emission directionality. This information allows to localize the birth place of the emitted particles and effectively suppress background from the surrounding detector components (electrodes and chamber wall). Additionally corrections in the energy of the observed reaction products can be made to compensate for loss of ionization electrons on electronegative gas admixtures and pulse height defect.

There is a number of advantages using gas targets in cross section measurements instead of solid ones: 1) the large number of target atoms. For a 3% content of the concerned isotope in the working gas we can get a 100 times larger number of atoms in comparison with a typical few ten  $\mu\text{g}/\text{cm}^2$  solid target situated on the cathode; 2) the freedom of determining an isolated target cell inside the detector's sensitive volume. The latter allows to have an effective suppression of background from the surrounding detector components (electrodes and chamber wall); 3) most of the light gases are not radioactive and the determination of the number of atoms is not a simple task. For a set of elements, such as noble gases Ne, Ar and others, the preparation of solid targets is problematic due to their physical and chemical properties. Use of gaseous targets solves these problems. The number of atoms in a gaseous target can be determined using the simple laws valid for ideal gases; 4) the sum of the kinetic energies of both reaction products is measured and there is no passive energy loss as is the case using solid targets, where tedious corrections for energy loss in the sample and its

backing are required and additionally transformation of the angle dependent energy of single reaction products from the laboratory to centre-of-mass coordinate system has to be performed; 5) with a gas target the detector registers particles in the full  $4\pi$  solid angle. With a solid target a maximum solid angle of  $2\pi$  can be covered, so that two conventional GIC spectrometers, one for forward and one for backward emission with separate target samples and electronics, are needed for  $4\pi$  detection.

To produce fast neutrons at IPPE proton and deuterium beams and the (p,T) and (d,D) reactions were used, respectively, at the EG-1 accelerator. Solid deuterium and tritium targets with thickness from 1 to 2 mg/cm<sup>2</sup> were used.

The digitized fission fragment signals were used to generate a pulse height spectrum with a clean separation between neutron induced fission and natural  $\alpha$  particle decay. The settings of the cathode amplifier were optimised for  $\alpha$  particle detection in the GIC chamber. With these amplifier settings the fission fragment signals were saturated. This was not a problem because the purpose of the neutron monitor was to record only the number of fission events and not their real energy distribution. The total number of fission events was obtained by properly extrapolating the fission fragment spectrum to zero pulse height.

## 2 Results of the experimental investigation using gaseous targets

### 2.1 The cross section of the $^{16}\text{O}(n,\alpha)$ reaction.

In this experiment a 96.84%Kr+3.16%CO<sub>2</sub> gas mixture was used. The gas manufacturer (Linde) guaranteed the number of CO<sub>2</sub> with a precision better than 3%. The oxygen content was used as target for the study of the (n, $\alpha$ ) reaction. Investigation of the  $^{16}\text{O}(n,\alpha_0)$  reaction channel in the neutron energy range 1.7 – 7 MeV was made. The result is shown on figure 3. The IPPE data are in the good agreement with an earlier IRMM–IPPE data set [1] and the Harissopolos et al. [2] data. In the present work the energy range 5.2-6.2 MeV was investigated in more detail than in the earlier IRMM–IPPE work. Particularly the new data show a neutron energy point to the left of which there is good agreement with the ENDF/B-VII evaluation but to the right of it there is a large discrepancy by a factor of up to 1.8.

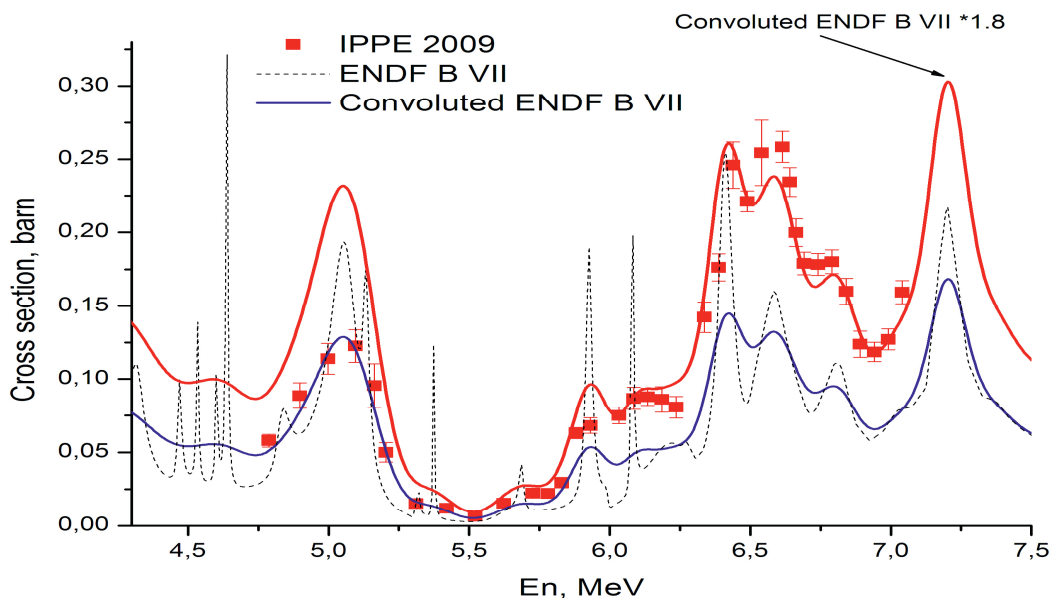


Fig 3. Energy dependence of the  $^{16}\text{O}(n,\alpha_0)$  cross section.

## 2.2 The cross section of the $^{14}\text{N}(n,\alpha)$ reaction.

In this measurement a 97%Kr+3%N<sub>2</sub> gas mixture was used. The precision for the number of the nitrogen atoms (3%) was provided by the gas producer. Nitrogen contained in the working gas was used as target for the (n,α) reaction and it is also assumed to be an admixture which increases the electron drift velocity. Investigation of the  $^{14}\text{N}(n,\alpha_0)$ ,  $^{14}\text{N}(n,\alpha_1)$  and  $^{14}\text{N}(n,\alpha_2)$  reaction channels in the neutron energy range 1.7 – 7 MeV was made. The result is shown in figure 4. As is shown our data are in good agreement with the ENDF/B-VII evaluation and Gabbard et al. [3] data in the energy ranges 1.7-3 and 6-7 MeV but in the energy range 4-6 MeV a large discrepancy by a factor of up to 3 and more exists. A possible explanation of this discrepancy was found by analysis of energy spectra. For the 4-6 MeV energy range there is a minimum for the cross section to the left of which there is a broad region with a very high cross section level. For this condition a small number of background neutrons (with low energy) can produce a lot of α particles. If the detector energy resolution is low this background will be added to the real events resulting in a measured cross section which has a larger value than the real one.

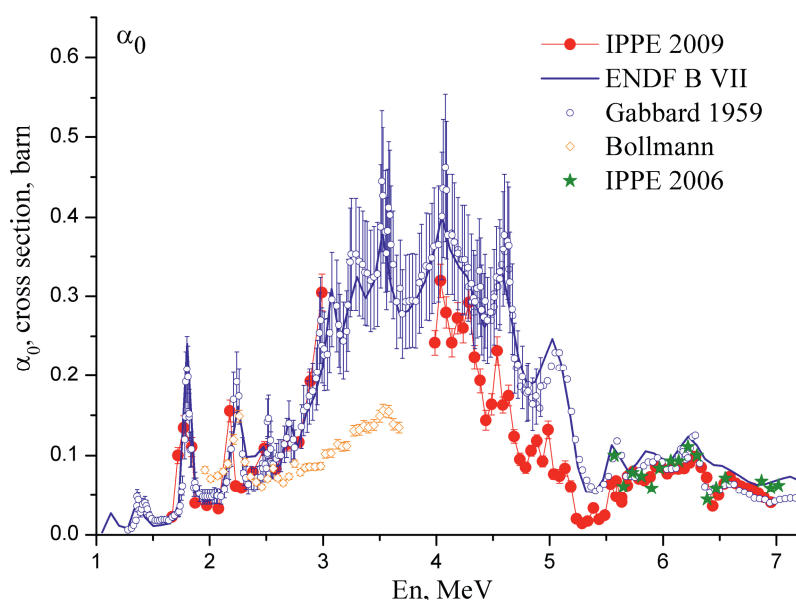


Fig 4. Energy dependence of the  $^{14}\text{N}(n,\alpha_0)$  cross section.

## 2.3 The cross section the of $^{20}\text{Ne}(n,\alpha)$ reaction.

In this measurement a 73.72%Kr+22.3%Ne+3.98%CO<sub>2</sub> gas mixture was used. The gas manufacturer (Linde) guaranteed the number of neon atoms with a precision better than 3%. Neon was used as target for the (n,α) reaction. Carbon dioxide was added to increase the electron drift velocity. Cross section data for the individual reaction channels  $^{20}\text{Ne}(n,\alpha_0)$ ,  $^{20}\text{Ne}(n,\alpha_1)$ ,  $^{20}\text{Ne}(n,\alpha_2)$  and  $^{20}\text{Ne}(n,\alpha_3)$  were obtained for the first time in the neutron energy range 4–7 MeV. We know of published measurements with unresolved α particle groups, so that only cross sections of grouped channels could be compared with other experimental data. The sum of the  $^{20}\text{Ne}(n,\alpha_0)$  and  $^{20}\text{Ne}(n,\alpha_1)$  cross section is shown in figure 5 together with the data of Bell et al. [4]. The IPPE cross sections have higher values by a factor of up to 3. A large influence of the pulse height defect was observed in the IPPE measurements. The right branch of the “V type” shape of the excitation function corresponds

to  $\alpha$  particles emitted in the direction of the neutron beam. The left branch corresponds to  $\alpha$  particles emitted opposite to the direction of the neutron beam. A similar effect was found in [4].

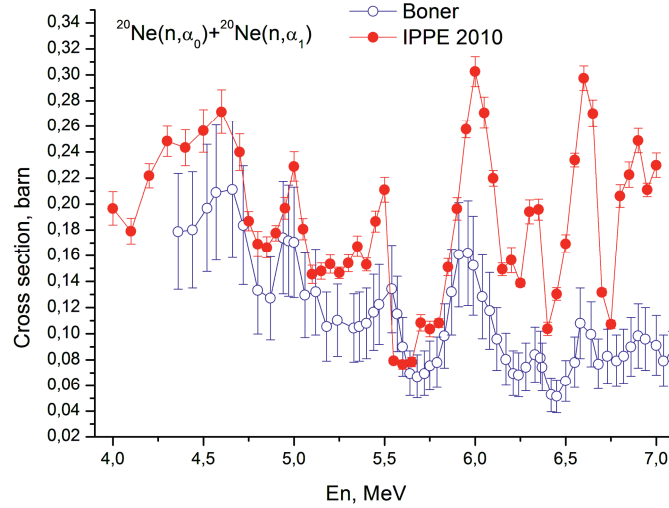


Fig 5. Energy dependence of the sum of the cross sections of the  $^{20}\text{Ne}(n,\alpha_0)$  and  $^{20}\text{Ne}(n,\alpha_1)$  reaction channels.

#### 2.4 The cross section of the $^{36}\text{Ar}(n,\alpha)$ and $^{40}\text{Ar}(n,\alpha)$ reactions.

In this measurement a P10(90%Ar+10%CH<sub>4</sub>) gas mixture was used. The gas manufacturer (Linde) guaranteed the number of argon atoms with a precision better than 3%. The argon in working gas was used as target for the study of the (n,α) reaction. In this experiment we did not use carbon dioxide to increase the electron drift velocity because the Q value of the  $^{16}\text{O}(n,\alpha_0)$  reaction is close to the one of  $^{40}\text{Ar}(n,\alpha_0)$ .

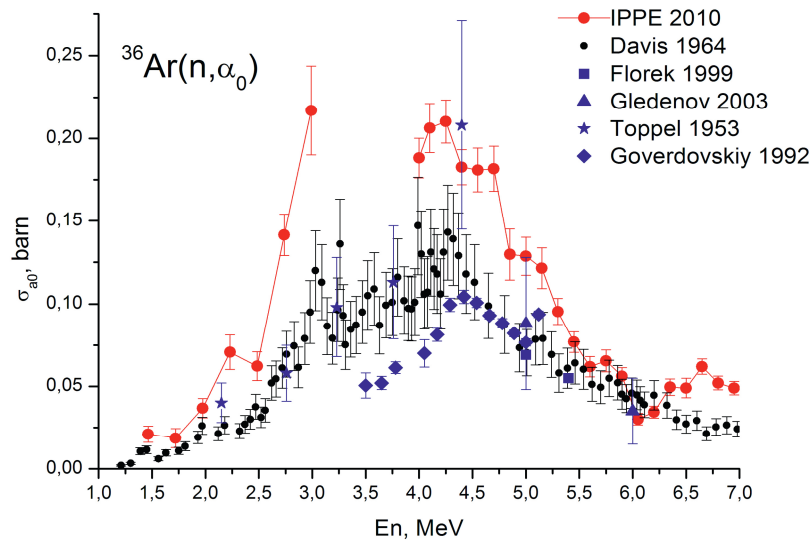


Fig 6. Energy dependence of the  $^{36}\text{Ar}(n,\alpha_0)$  cross section.

Methane was used instead, but in this case a lot of recoil protons were produced in the working gas. Use of digital methods for pulse shape analysis allowed a clear separation of recoil protons from  $\alpha$  particles. Investigation of the  $^{36}\text{Ar}(n,\alpha_0)$ ,  $^{36}\text{Ar}(n,\alpha_1)$  and  $^{40}\text{Ar}(n,\alpha_0)$  reactions in neutron energy range 1.5 – 7 MeV was made. Some of the results are shown in figures 6 and 7.

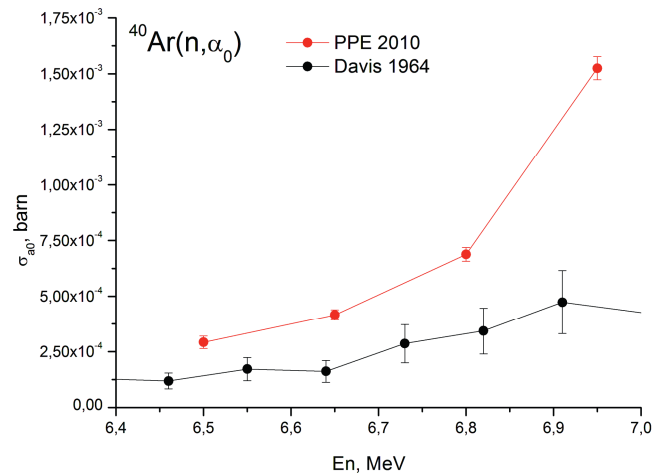


Fig 7. Energy dependence of the  $^{40}\text{Ar}(n,\alpha_0)$  cross section.

A large discrepancy by a factor of up to 2 was observed in the full energy range between our cross sections and the data of Davis et al. [5]. In contrast to other reactions investigated by Davis et al. this reaction has a large positive Q-value. For this condition the wall effect is much larger than in the other cases. We assume therefore that the theoretical calculation of the wall effect correction which was made in [5] is of low accuracy so that an underestimation of this correction could be the reason for the discrepancy.

## 2.5 The branching ratio $\alpha_0/\alpha_1$ of the $^{10}\text{B}(n,\alpha)$ reaction.

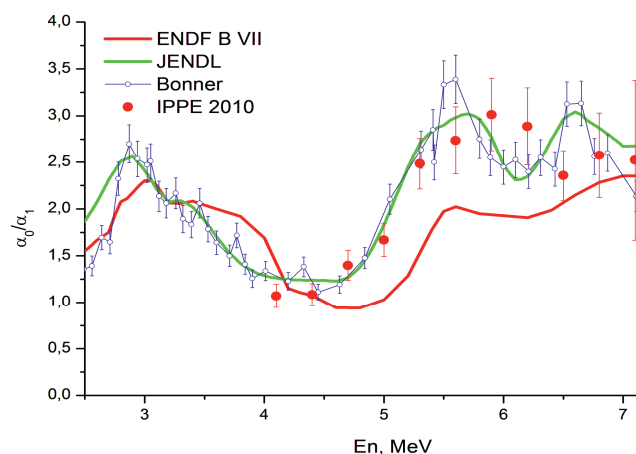


Fig 8. Energy dependence of the branching ratio  $\alpha_0/\alpha_1$  of the  $^{10}\text{B}(n,\alpha)$  reaction.



In this measurement a Kr+10%BF<sub>3</sub> gas mixture was used. Boron trifluoride is a pungent, toxic and strongly electronegative gas. Water of 1 g (1 ml) at 0°C and 762 mm Hg absorbs 3.76 g BF<sub>3</sub> (1 ml H<sub>2</sub>O absorbs 1242 ml of gaseous BF<sub>3</sub>). To make with this gas work possible the chamber and gas system had to undergo major modifications. Furthermore a special algorithm was incorporated in the evaluation programs allowing corrections for electron capture in the working gas. All these improvements allowed to work safely with boron trifluoride and to achieve a reasonable energy resolution. It is necessary to notice that measurement of the yield ratio using a gaseous target is practically free of systematic uncertainties.

Yield ratios do not depend on the working gas pressure, number of boron atoms and isotopic composition. They also do not depend on the selection of a gaseous target inside the GIC sensitive volume. The results of the IPPE measurement together with different evaluations and the Davis et al. [6] data are shown in figure 8. The IPPE data are in good agreement with those of the Davis et al. As can be seen there is a significant difference between the ENDF/B-VII and JENDL evaluations. The IPPE data are clearly in better agreement with JENDL than with ENDF/B-VI in the 4-7 MeV energy range.

### 3 The cross section of the <sup>50</sup>Cr(n,α) reaction

#### 3.1 Experimental set up

In this measurement a chromium solid target with 96.8% of Cr-50 was used. The Content of other isotopes is: Cr-52 - 2.98%, Cr-53 - 0.18%, and Cr-54 - 0.04%. The total target mass was 5.15 mg. The chromium target had a gold foil backing of 84 mg/sm<sup>2</sup> thickness and was installed in an gridded ionization chamber filled with a 97%Kr+3%CH<sub>4</sub> gas mixture at 3 atmosphere pressure. Use of methane gas in the detector working in a high energy neutron field led to huge recoil proton background. Though, an attempt to use a Kr+CO<sub>2</sub> gas mixture produced a very disturbing α particle background due to the <sup>16</sup>O(n,α) reaction. Finally we found out that it was easier to separate <sup>50</sup>Cr(n,α) events from numerous recoil protons than from rare α-particles by using signal digital processing.

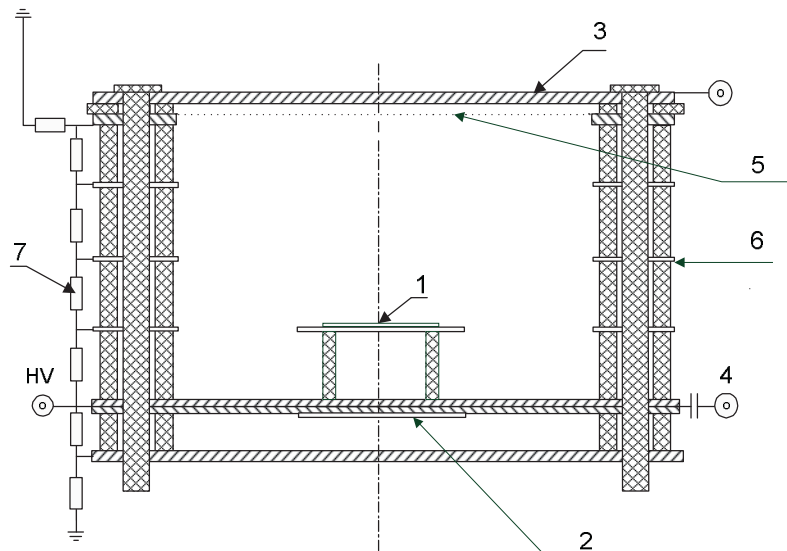


**Fig 9.** Diagram of GIC. 1- target <sup>50</sup>Cr; 2 – target <sup>238</sup>U; 3 – GIC anode; 4 – common cathode; 5 – Frisch grid; 6 – guarding electrodes ; 7 – divider.



The first experience of placing the chromium target on the cathode showed intense emission of  $\alpha$  particles from  $(n,\alpha)$  reactions on components of the cathode material. The authors have enough experience in making investigations of  $(n,\alpha)$  reactions on working gas components [1]. Following this first test the target was placed in some distance from the cathode and facing the grid as shown in figure 9. Under these conditions it was possible to separate  $\alpha$ -particles arising in target from those produced at the cathode or in the working gas. Such a detailed analysis of cathode and anode signals could be realized only by applying digital signal processing.

### 3.2 Results

Our measurement results together with different evaluations and the Baba et al. [7] data are shown in figure 10. It is absolutely clear that our data are in significant disagreement with the ENDF/B-VII evaluation. For some energies the ENDF/B-VII-to-the experimental cross section ratio rises up to 50 times. The JENDL evaluation is in better agreement compared to the IPPE data, with the latter being systematically lower than the JENDL values except around 6 MeV, the region of a structure in the IPPE data, which is absent in the JENDL excitation function.

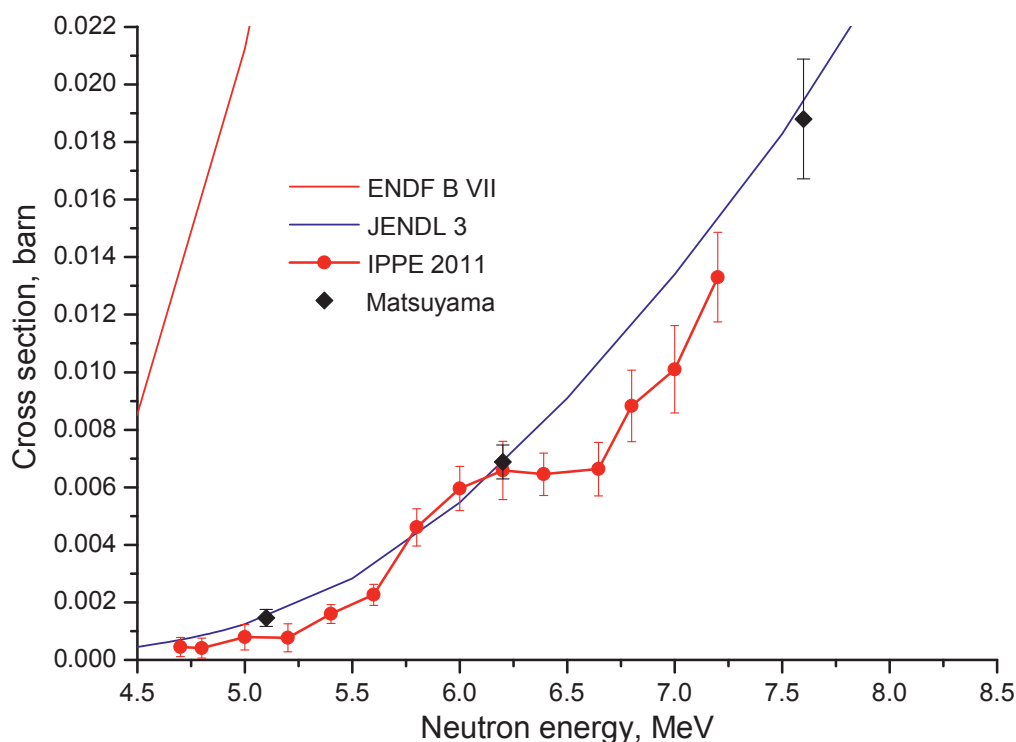


Fig 10. Energy dependence of the  $^{50}\text{Cr}(n,\alpha)$  cross section.

### 4 Future plans.

Currently we are continuing measurements with  $^{10}\text{B}$  at lower neutron energies. In the near future we plan to measure the  $^{19}\text{F}(n,\alpha)$  and  $^{12}\text{C}(n,\alpha)$  cross sections. Furthermore we have developed and now we are finishing with the manufacturing of a new low background spectrometer which will allow to investigate  $(n,\alpha)$  reactions on solid targets for Li and structural elements such as Fe, Ni, Cr, V and others.

## 5 Conclusion

It was shown that a new digital spectrometer with a gaseous target allowed to measure  $(n,\alpha)$  cross sections with high precision. Published work so far shows that in spite of a long time history of investigation of  $(n,\alpha)$  reactions on light elements the uncertainty of the cross section was till recently on the level of a few to several ten of hundred percent.

Common conclusion of the present work is that the existing estimation of  $(n,\alpha)$  cross section can not describe the real situation. To solve this problem there is a need for new experimental data and new efforts on the side of theoretical investigations.

## References

1. G. Giorginis, V.Khryachkov, V. Corcalciuc, M. Kievets, *In Proc. Of Int. Conf. NDST 2007 conference, Nice, 525* (2007).
2. S.Harissopulos, H.W.Becker et al., *Phys. Rev. C* **72**, 062801 (2005).
3. F.Gabbard, H.Bichsel, T.W.Bonner, *Nucl. Phys.* **14**, 277 (1959/1960).
4. R.J.Bell, T.W.Bonner, F.Gabbard, *Nucl. Phys.* **14**, 270 (1959/1960).
5. E.A.Davis, T.W.Bonner, D.W.Worley, R.Bass, *Nucl. Phys.* **55**, 643 (1964).
6. E.A.Davis, F.Gabbard, T.W.Bonner, R.Bass, *Nucl. Phys.* **27**, 448 (1961).
7. M. Baba, N. Ito, I. Matsuyama, S. Matsuyama, N. Hirakawa, S. Chiba, T. Fukhori, M. Mizumoto, K. Hasegawa, S. I. Meigo, *In Proc. of the International Conference on Nuclear Data for Science and Technology, Gatlinburg, 941* (1994).